Progress In Electromagnetics Research, PIER 66, 111–124, 2006

DESIGN OF WIDE-BAND DIELECTRIC RESONATOR ANTENNA WITH A TWO-SEGMENT STRUCTURE

P. Rezaei, M. Hakkak, and K. Forooraghi †

Faculty of Engineering
Department of Electrical Engineering
Tarbiat Modares University (TMU)
Tehran, Iran

Abstract—This paper discusses the analysis of a novel two-segment rectangular dielectric resonator antenna (DRA) for broadening of the impedance bandwidth. In the proposed configuration, two rectangular dielectric sections are used which are separated by a metal plate. With this configuration, it is possible to excite two adjacent resonant frequencies. Utilizing the two-segment thin DRA and skillfully varying its aspect ratio, an appropriate structure is obtained that illustrates more than 76.8% impedance bandwidth (for S_{11}>10 dB) at 3.32–7.46 GHz frequency band.

1. INTRODUCTION

The dielectric resonator (DR) is fabricated from low-loss dielectric materials. Its resonant frequencies are predominantly a function of size, shape, and material permittivity. DRs offer the advantages of small size, lightweight, low profile, and low cost. They have been demonstrated to be practical elements for antenna applications and have several merits including high radiation efficiency, flexible feed arrangement, simple geometry, and compactness [1, 2].

The antenna applications of DRs were first proposed in the early 1980's [3]. Later, various investigations offered significant enhancements to parameters such as bandwidth, gain, polarization, or coupling [4–7]. Over the last decades, various bandwidth enhancement techniques have been developed for DRAs. These techniques were classified into three categories: Lowering the inherent Q-factor of the

† The first and second authors are also with Iran Telecommunication Research Center (ITRC), Tehran, Iran.

resonator, using external matching networks and combine multiple DRs [4].

DRAs are commonly available in rectangular, cylindrical, and hemispherical geometries. Rectangular DRAs offer more design flexibility since two of the three of its dimensions can be varied independently for a fixed resonant frequency and known dielectric constant of the material [8].

In this paper, a two-segment rectangular dielectric section in a suitable arrangement is used to enhance the bandwidth of DRA. This structure is composed of two rectangular sections with different (size and permittivity) which are separated by a perfect E plate [9].

Formerly, the overlap multi-segment DRA was developed to enhance coupling from the microstrip line [10, 11]. But the proposed arrangement emphasizes the bandwidth broadening and size reduction of the DRA.

The purpose of this investigation is to attempt to design DRAs that are sufficiently compact and in addition have proper impedance bandwidth for use in broadband communications.

2. HALF VOLUME DRA

By using an extra metallic plate in a conventional DRA, which acts as an electric wall, the size of the DRA has been reduced approximately by half [12–16]. The added plate acts as a shorting post for the electric field and allows part of the DRA to be removed, if certain field symmetry exists. The use of the metal plate can be compared to the shortening post used in patch antennas to reduce their length from $\lambda/2$ to $\lambda/4$ [12].

Because of the symmetry of EM field distribution in the main resonance frequency, we can divide the DRA into two halves with a metallic plate with zero thickness, perpendicular to the conducting ground plane. The field distribution in the other half remains unchanged in the main resonance case, and we can expect the resonant frequency to remain the same. In this case the volume of the DRA is effectively reduced by half. Greater reductions (as high as 75%) in the volume of the DRA can also be obtained by utilizing sectored structures [17]. However, the feed setup (ΔL) is expected to need alteration to give a good impedance match for the half volume design.

This is the base of our idea to obtain volume reduction and wide bandwidth of operation. To this purpose we consider Figure 1.

What we are looking for, is a DRA that can offer different resonant frequencies. The two half DRAs, due to their different permittivity and size, resonate in two different frequencies. These two frequencies can

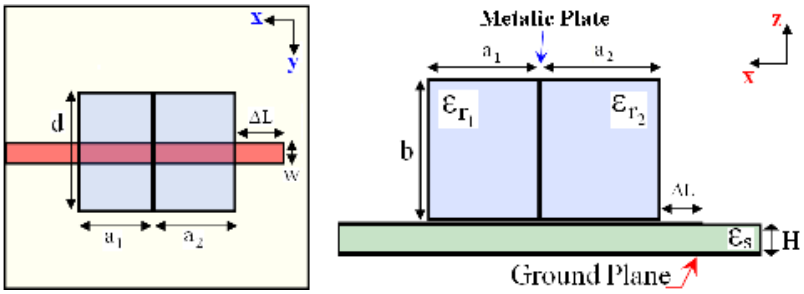

(a) (b)

Figure 1. Geometry of proposed antenna fed by microstrip line (a) top and (b) profile view.

be merged so that it can be used for wideband applications [9].

By letting the two resonant frequencies from the two segments being f_1 and f_2 with $f_1 < f_2$ (for $a_1 > a_2$), the merged frequency band condition is fulfilled when

$$f_1 + \frac{\Delta f_1}{2} \geq f_2 - \frac{\Delta f_2}{2} \tag{1}$$

where Δf is the 3-dB bandwidth of S_{11} curve. By choosing suitable values of a_1 and a_2 lengths such that Eq. (1) with an equality symbol is satisfied, a broad continuous impedance bandwidth is achieved. For this purpose, the effects of a_1 and a_2 on the input impedance and consequently on the matched bandwidth are investigated on the finite ground plane.

Full wave analysis of the proposed antenna configurations were performed using Ansoft HFSS^{TM} [18] based on finite element method. In addition, the simulation results of CST Microwave Studio [19], based on finite integral technique, are provided to support our findings from HFSS software.

More than one metal plate can be added to obtain the required impedance match, but to reduce the complexity of the fabrication process and cost; it is desirable to use only a single plate [10]. Moreover, because of the additional metallic plates, a decrease in radiation efficiency will occur.

3. STRUCTURE DESIGNS AND SIMULATIONS

Extensive simulations were carried out using the software in order to obtain optimal design parameters for the antenna. The initial

dimensions of the radiating portions of the antenna were determined using the equations developed for the dielectric waveguide model (DWM) for a rectangular resonator in free space [8].

Enforcing the magnetic wall boundary condition at the surfaces of the resonator, the following equations are obtained for the wave-numbers and the dominant mode resonance frequency:

$$k_x^2 + k_y^2 + k_z^2 = \varepsilon_r k_0^2 \tag{2}$$

$$f_0 = \frac{c}{2\pi\sqrt{\varepsilon_r}}\sqrt{k_x^2 + k_y^2 + k_z^2} \tag{3}$$

where

$$k_x = \frac{\pi}{a}, \quad k_y = \frac{\pi}{b}, \quad k_z tag(k_z d/2) = \sqrt{(\varepsilon_r - 1)k_0^2 - k_z^2} \tag{4}$$

where k_x, k_y, and k_z denote the wave-numbers along the x, y, and z directions inside the DR, respectively. Then the appropriate dimensions of the antenna parameters were determined with trial optimization.

In general, to achieve strong coupling, the DRA must be fabricated from high permittivity materials. But, to operate over a wide bandwidth, the DRA must have a low dielectric constant [1]. Previous work has shown the critical coupling is possible for DRAs having a high value (20 or much) of dielectric constant [8]. The two segments are made of the same material with a dielectric constant of $\varepsilon_r = 20$.

3.1. Parametric Study

The microstrip feed-line is 1mm wide and on a 0.33 mm thick substrate with a relative dielectric constant, $\varepsilon_s = 2.2$, to give a characteristic impedance of 50Ω. Open circuit microstrip line is considered to excite the DR. To achieve the maximum coupling, the DRA is placed at a distance of $\lambda/2$ from the open end [8]. For this case the finest coupling and consequently the maximum bandwidth for $\Delta L = 4.1$ mm was achieved.

The dimensions ($a \times d \times b$) of the proposed DRA are 10.5 mm × 6 mm × 9.6 mm that are equivalent to $0.192\lambda \times 0.11\lambda \times 0.176\lambda$ and λ is the free space wavelength at the center frequency of 5.5 GHz. Additionally, the proper lengths of the two segments (a_1 and a_2) are obtained 4.8 mm, and 5.7 mm respectively. The size of square ground plane is assumed to be 50 mm × 50 mm.

To compare the effects of variation in lengths of the two segments (a_1 and a_2), different arrangements of these lengths were evaluated.

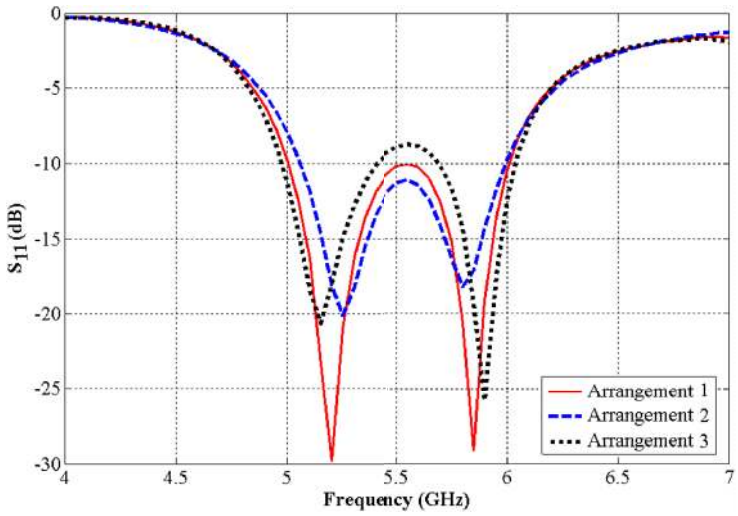

Figure 2. Return loss of different arrangement of the two-segment DRA.

For example, return loss for a_1 and a_2 (4.6 mm and 5.9 mm) and (5 mm and 5.5 mm) are shown in Figure 2, labeled as "arrangement 2" and "arrangement 3", respectively.

Eq. (1) is satisfied in arrangement 1 and consequently wider impedance bandwidth is realized in this case. In arrangement 2, due to closeness of the two resonant frequencies, the impedance bandwidth is limited to 16.83%. Likewise, arrangement 3 has two separated bands, which offer 14.44% bandwidth totally.

The associated input impedance and return loss curves of the designed two-segment DRA are shown in Figures 3a and 3b respectively.

The simulated results (HFSS software) have shown two resonant frequencies at 5.2 GHz and 5.84 GHz and impedance bandwidth at 5.01–6.01 GHz, which illustrates more than 18.1% frequency bandwidth.

The returns loss curves for two configurations, single and two-segment structures, with the same dimensions are compared in Figure 3b. Also, the results of the HFSS simulations are grossly confirmed by using simulation results from CST Microwave Studio with the same setup as mentioned above. The obtained results are illustrated in Figure 3b, as well.

The comparative simulation results for one- and two-segment

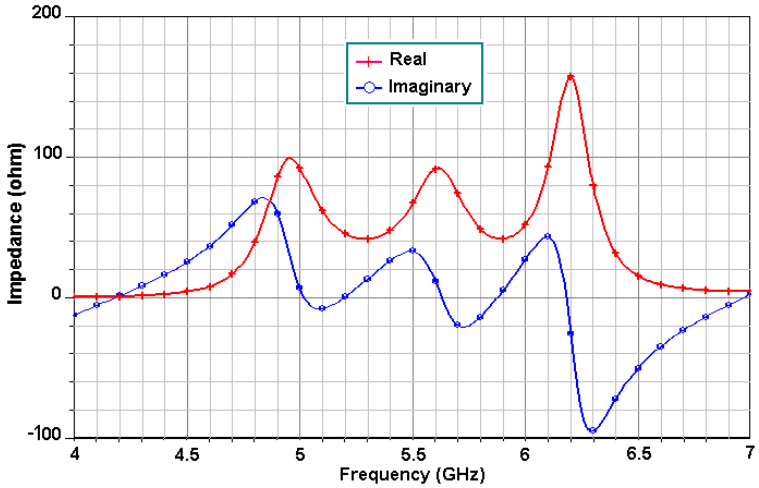

Figure 3a. Input impedance curve of the two-segment DRA.

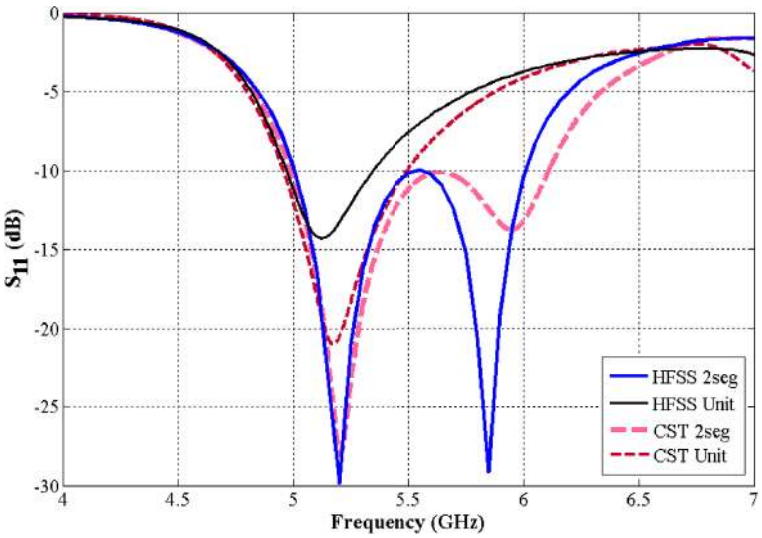

Figure 3b. Comparison of return loss between single and two-segment DRAs, simulated with HFSS and CST Microwave Studio software.

DRAs, from both software programs, are listed in Table 1.

Table 1. Resonant frequency and impedance bandwidth for single and two-segment of DRA obtained with HFSS and CST microwave studio simulations.

DRA Structure	Parameter (GHz)	HFSS	CST-MS
Single	Resonant freq.	5.12	5.17
	Bandwidth	4.96-5.36 (7.75%)	4.96-5.49 (10.13%)
2 Segment	Resonant freq.	5.19 & 5.84	5.20 & 5.95
	Bandwidth	5.01-6.01 (18.15%)	4.99-6.11 (20.18%)

In the proposed structure the impedance bandwidth have been increased more than 100%, in comparison with single structure without insulator plate.

This two-segment DRA is proposed for WLAN systems [9]. With regard to IEEE 802.11a standard, a single-band antenna designed for this system should therefore work at center frequency 5487.5 MHz and bandwidth 675 MHz (5150–5825 MHz) or 12.3% [9, 20]. The obtained bandwidth is easily meeting this system requirement.

Moreover, another advantage of the proposed structure is that it offers two optimum locations for antenna on the ground plane by readjusting the ΔL length after rotating the antenna in the feed-line direction. In above case, by pivoting the antenna (i.e., exchanging the position of a_1 and a_2), the optimum return loss curve for $\Delta L = 6.1$ mm is obtained (see Figure 4).

In this case, the bandwidth has slightly narrowed and has shifted to higher frequencies, and the resonant frequencies have shifted to 5.34 GHz and 5.90 GHz. Also, the impedance bandwidth has shifted to 5.08–6.06 GHz with 17.59% bandwidth. This bandwidth still satisfies the WLAN system specifications mentioned earlier.

Afterward, the far-field radiation patterns of DRA structures were investigated. The resulting three dimensional (3-D) radiation patterns at 5.5 GHz for single and two-segment structures are shown in Figures 5a and 5b, respectively.

The single segment DRA has a symmetrical pattern respect to x-z and y-z planes (see Figure 5a). In the two-segment structure due to the metal plate, as shown in Figure 5b, radiation pattern has a main lobe in minus x-axis direction.

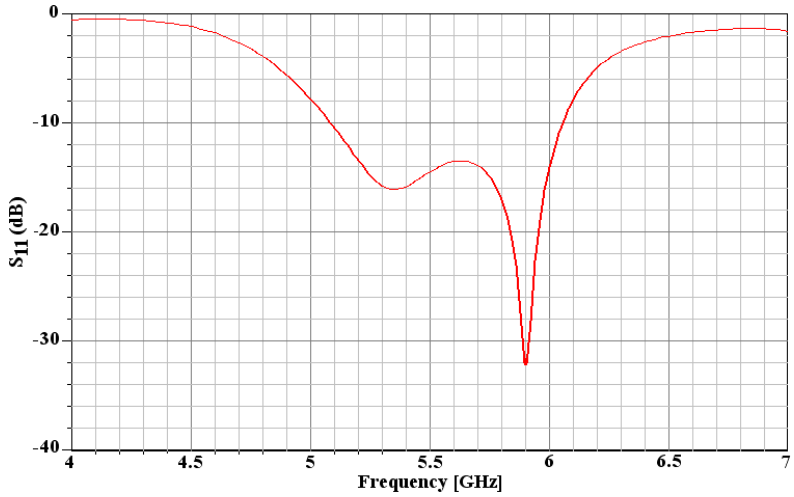

Figure 4. Return loss of the pivoted two-segment DRA.

4. DESIGN OF WIDEBAND DRA

In this section, to obtain better results, the antenna dimensions have been enhanced. Greater improvements in bandwidth can be achieved by suitable selection of aspect ratio. For this reason, a scheme like what was used for the cylindrical DRA is applied. In cylindrical structure, the resonant frequency of the modes can be adjusted by the radius

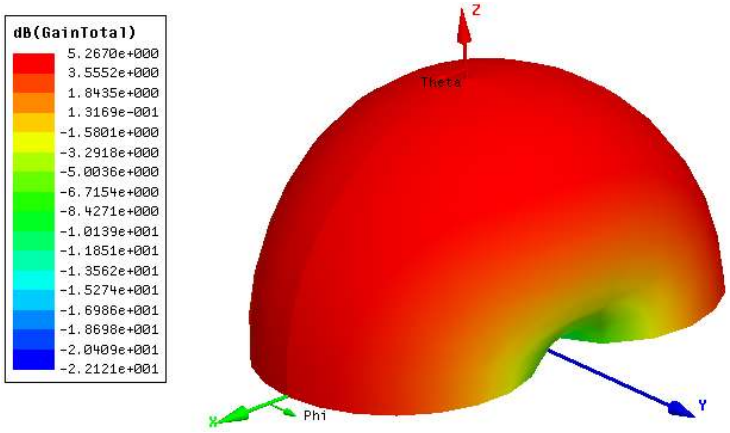

Figure 5a. 3-D radiation pattern of single DRA structure at 5.5 GHz.

to height ratio of the cylindrical DRA. A wide bandwidth is reported when this ratio equals to 0.329 [21].

Also in pervious works have been shown that thin transverse structure exhibit wider bandwidth. In fact, increase in height to width ratio (b/d) results in a significant increase in the bandwidth. Hereunder, the structures with higher b/d ratios are evaluated and compared to the structures evaluated in the previous section. Also in the feed-line, the far end of a microstrip line is terminated in an open circuit.

The dimensions (a, d, and b) of this proposed DRA are 10.8 mm by 2.56 mm by 12.8 mm high which are equivalent to 0.198λ by 0.047λ by 0.235λ high where λ is the free space wavelength of 5.5 GHz. The optimum lengths of a_1 and a_2 are obtained 4.9 mm, and 5.9 mm respectively.

A general expression linking the unloaded Q to the antenna basic geometrical features is [23]:

$$Q = 2\omega_0 \frac{\text{Stored Energy}}{\text{Radiated Power}} \propto 2\omega_0 \varepsilon_r^p \left(\frac{\text{Volume}}{\text{Surface}}\right)^s \quad \text{with } p > s \geq 1 \quad (5)$$

In the thin structure, the volume to surface ratio (V/S) is decreased about 34.8% compared to the first design (from 1.366 to 0.891). Therefore, with reference to Eq. (5), we expect that the Q-factor is decreased and consequently the bandwidth is increased. The associated input impedance and return loss curves of the second designed two-segment DRA are shown in Figures 6 and 7 respectively.

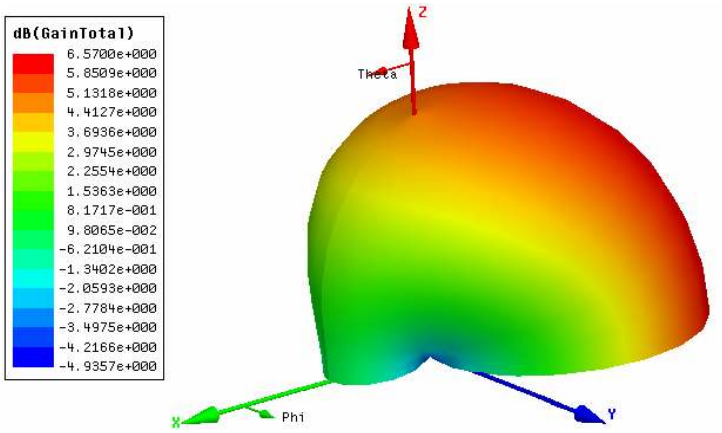

Figure 5b. 3-D radiation pattern of the two-segment DRA structure at 5.5 GHz.

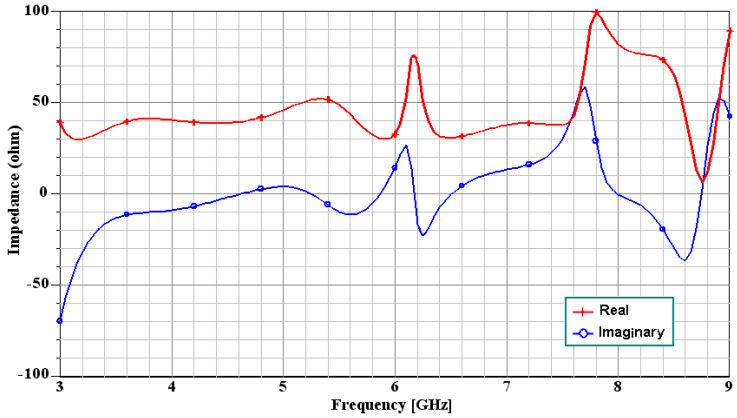

Figure 6. Input impedance of the thin two-segment DRA.

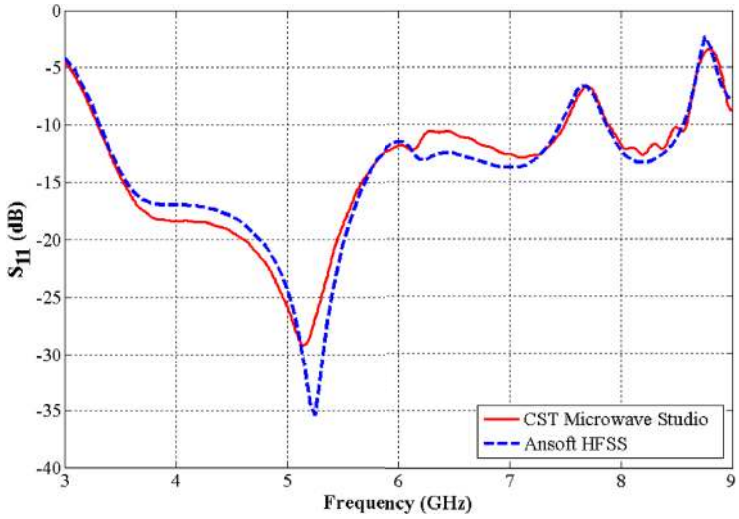

Figure 7. Comparison of return loss of the thin two-segment DRA, simulated with HFSS and CST Microwave studio software.

In Figure 6, the same as Figure 3a, the real and imaginary parts of the impedance curve swing around 50 and 0 Ω, respectively, to provide acceptable impedance matching with the feed-line.

For the optimum thin DRA, the simulation results of HFSS show matched impedance bandwidth at 3.32–7.46 GHz band, illustrating more than 76.8% frequency bandwidth. Also, simulation results of CST Microwave Studio show matched impedance bandwidth at 3.31–

Table 2. Dimensions, aspect ratio, and impedance bandwidth for 2 proposed scheme of the two-segment DRA obtained with simulations.

Scheme	Dimensions (mm)					Volume (mm^3)	V/S	Bandwidth %	
	a_1	a_2	d	b	b/d			HFSS	CST
First	4.8	5.7	6	9.6	1.6	604.8	1.366	18.15	20.18
Second	4.9	5.9	2.56	12.8	5	353.89	0.891	76.81	77.41

7.49 GHz band, i.e., more than 77.4% frequency bandwidth. Good agreement between the two software simulations is obtained for the entire bandwidth. In Table 2, dimensions, volume, aspect ratio, and bandwidth results from HFSS and CST Microwave Studio simulations for both of the designed antennas are provided.

The second scheme, the thin structure, occupies 41.5% less volume compared to the first DRA.

In wideband scheme, DRA operates with different modes over the entire impedance bandwidth, and consequently we have different far-field radiation patterns. The boresight gain curve, with three typical 3-D radiation patterns at 3.5, 6.5, and 8 GHz are shown in Figure 8.

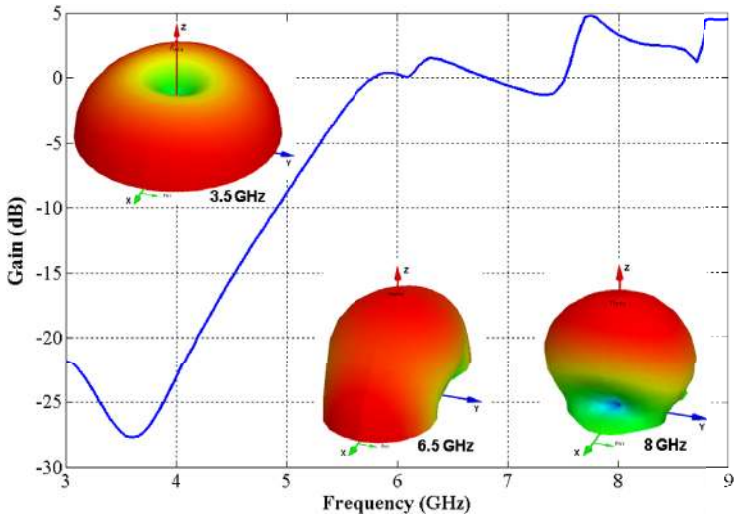

Figure 8. The boresight gain of the thin two-segment DRA, with three typical radiation patterns at 3.5, 6.5, and 8 GHz.

As shown in Figure 8, in lower frequency band, the pattern has a main-lobe in x-y plane and a null in z direction. In the upper frequency

band, the pattern is semi-hemispherical with a main-lobe in z direction. Moreover, Figure 8 shows 3-dB gain bandwidth in 5.5–7.5 GHz band, i.e., 30.76% frequency bandwidth.

From a number of simulations we have found that CST microwave studio simulations generally predict wider frequency bandwidth than HFSS simulations with the same structure. Also, in our simulations we have found that with a constant volume, the special b/d ratios of around 5 provide the widest frequency bandwidth.

5. CONCLUSIONS

In this work, a two-segment rectangular DRA structure separated by a metal plate was introduced, and performance of this structure was analyzed. In comparison to a single DRA, this structure offers a significant reduction of 41.5% in volume. Therefore, such a structure is a potential candidate for use in compact and wideband applications. In the suggested thin DRA with a suitable aspect ratio, an impedance bandwidth of 3.32–7.46 GHz is obtained, which is equivalent to a frequency bandwidth of as high as 76.8% (for S_{11}>10 dB).

ACKNOWLEDGMENT

This work was supported by the Iran Telecommunication Research Center. The authors also express their appreciation to Mr. A. Pirhadi and Mr. F. Hakkak, for valuable advices.

REFERENCES

1. Petosa, A., A. Ittipiboon, Y. M. M. Antar, and D. Roscoe, "Recent advances in dielectric resonator antenna technology," *IEEE Antennas and Propagation Magazine*, Vol. 40, No. 3, 35–48, June 1998.
2. Mongia, R. K. and P. Bhartia, "Dielectric resonator antennas — A review and general design relations for resonant frequency and bandwidth," *International Journal of Microwave Millimeter-Wave Engineering*, Vol. 4, 230–247, July 1994.
3. Long, S. A., M. W. McAllister, and L. C. Shen, "The resonant cylindrical dielectric cavity antenna," *IEEE Trans. on Antennas and Propagation*, Vol. 31, No. 3, 406–412, May 1983.
4. Luk, K. M. and K. W. Leung, *Dielectric Resonator Antennas*, Research Studies Press LTD., London, 2003.

5. Rao, Q., T. A. Denidni, A. R. Sebak, and R. H. Johnston, "On improving impedance matching of a CPW fed low permittivity dielectric resonator antenna," *Progress In Electromagnetics Research*, PIER 53, 21–29, 2005.
6. Kumar, A. V. P., V. Hamsakutty, J. Yohannan, and K. T. Mathew, "Microstripline fed cylindrical dielectric resonator antenna with a coplanar parasitic strip," *Progress In Electromagnetics Research*, PIER 60, 143–152, 2006.
7. Qian, Z. H., K. W. Leung, and R. S. Chen, "Analysis of circularly polarized dielectric resonator antenna excited by a spiral slot," *Progress In Electromagnetics Research*, PIER 47, 111–121, 2004.
8. Mongia, R. K. and A. Ittipiboon, "Theoretical and experimental investigations on rectangular dielectric resonator antennas," *IEEE Tran. on Antennas and Propagation*, Vol. 45, No. 9, 1348–1356, September 1997.
9. Rezaei, P., M. Hakkak, and K. Forooraghi, "Dielectric resonator antenna for wireless LAN applications," *IEEE Antennas and Propagation Society International Symposium*, Vol. 2, 1005–1008, July 2006.
10. Petosa, A., N. Simons, R. Siushansian, A. Ittipiboon, and M. Cuhaci, "Design and analysis of multisegment dielectric resonator antennas," *IEEE Trans. on Antennas and propagation*, Vol. 48, No. 5, 738–742, May 2000.
11. Rashidian, A., K. Forooraghi, and M. Tayfeh-Aligodarz, "Investigations on two-segment dielectric resonator antennas," *Microwave and Optical Technology Letters*, Vol. 45, No. 6, 533–537, June 2005.
12. Tam, M. T. K. and R. D. Murch, "Half volume dielectric resonator antenna designs," *Electronics Letters*, Vol. 33, No. 23, 1914–1916, November 1997.
13. Saed, M. and R. Yadla, "Microstrip-fed low profile and compact dielectric resonator antennas," *Progress In Electromagnetics Research*, PIER 56, 151–162, 2006.
14. Juntunenl, J., O. Kiveka, J. Ollikainen, and P. Vainikainen, "FDTD simulation of a wide-band half volume DRA," *5th International Symposium on Antennas, Propagation and EM Theory*, 223–226, August 2000.
15. O'Keefe, S. G., S. P. Kingsley, and S. Saario, "FDTD simulation of radiation characteristics of half-volume HEM and TE-mode dielectric resonator antennas," *IEEE Trans. on Antennas and Propagations*, Vol. 50, No. 2, 175–179, February 2002.

16. Kishk, A. A. and A. W. Glisson, "Bandwidth enhancement for split cylindrical dielectric resonator antennas," *Progress In Electromagnetics Research*, PIER 33, 97–118, 2001.
17. Tam, M. T. K. and R. D. Murch, "Compact circular sector and annular sector dielectric resonator antennas," *IEEE Trans. on Antennas and Propagations*, Vol. 47, No. 5, 837–842, May 1999.
18. HFSS: High frequency structure simulator based on the finite element method, v. 9.2.1, Ansoft Corporation, 2004.
19. CST GmbH 2003 CST MICROWAVE STUDIO(r) User Manual V. 5.0, Darmstadt, Germany (www.cst.de).
20. Lan, K., S. K. Chaudhuri, and S. Safavi-Naeini, "A compact wide-dual-band antenna for bluetooth and wireless LAN applications," *IEEE Antennas and Propagation Society International Symposium*, Vol. 2, 926–929, June 2003.
21. Chair, R., A. A. Kishk, and K. F. Lee, "Wideband simple cylindrical dielectric resonator antennas," *IEEE Microwave and Wireless Components Letters*, Vol. 15, No. 4, 241–243, April 2005.
22. Cooper, M., "Investigation of current and novel rectangular dielectric resonator antennas for broadband applications at l-band frequencies," Master of Engineering Thesis, Carleton University, Ottawa, Canada, 1997.
23. Bit-Babik, G., C. Di-Nallo, and A. Faraone, "Multimode dielectric resonator antenna of very high permittivity," *IEEE Antennas and Propagation Society International Symposium*, Vol. 2, 1383–1386, June 2004.